Supplementary Information

for

Aqueous-phase Photochemical Oxidation of Water-Soluble Brown Carbon Aerosols Arising from Solid Biomass Fuel Burning

Vikram Choudhary[1, 2], Max Loebel Roson[1], Xinyang Guo[1], Tania Gautam[1], Tarun Gupta[2, *], and Ran Zhao[1, *]

[1]Department of Chemistry, University of Alberta, Edmonton-T6G 2R2, Alberta (Canada), [2]Department of Civil Engineering and APTL at Center for Environmental Science and Engineering (CESE), Indian Institute of Technology Kanpur, Kanpur - 208 016, India.

[*] Corresponding author: Tarun Gupta (tarun@iitk.ac.in), Ran Zhao (rz@ualberta.ca)

Number of pages: 25

No of Tables: 6

No. of Figures: 11

Section S1. Determination of Photon Flux

Photon flux indicates the absolute number of photons or light reaching the molecules present inside the aqueous solution in the photoreactor. The photon flux spectrum from 260 to 400 nm was determined in this study. Chemical actinometry of 2-nitrobenzaldehyde (2NB) was employed to determine photon flux for different UV-lights, *viz.*, UVB in quartz and glass vessel, expressed as UVB(Q) and UVB(G), respectively and UVA in quartz vessel (UVA(Q)) in the photoreactor. 2NB was chosen because it is thermally stable and its direct photolysis is well understood.[1] The direct photolysis rate of 2NB (J_{NB}), expressed in sec^{-1}, can be simulated using following equation:[1,2]

$$J_{NB}\,(sec^{-1}) = \frac{2.303 \times 10^{3}}{N_A} \int_{\lambda_{min}}^{\lambda_{max}} I_{\lambda}^{'} \times \phi(\lambda) \times \sigma(\lambda) \times d\lambda \qquad \text{Eq. S1}$$

where N_A is Avogadro's number, $I_{\lambda}^{'}$ is the photon flux spectrum (photons $cm^{-2}s^{-1}nm^{-1}$), dλ is wavelength interval between flux data points (nm), ϕ(λ) and σ(λ) are quantum yield (molecule $photon^{-1}$) and base-10 molar absorptivity ($M^{-1}cm^{-1}$) of 2NB, respectively. ϕ(λ) of 0.41 was used for all UV-lights discussed above as ϕ(λ) has been reported to be spectrally independent in the wavelength spectrum ranging from 260 to 400 nm.[1] σ(λ) of 2NB changes rapidly with wavelength and adopted from a previous study.[1] $I_{\lambda}^{'}$ for all UV-lights in the photoreactor was determined using a combination of direct emission spectra measurement and 2NB based chemical actinometry. Firstly, the direct measurement of emission spectra of all UV-lights was carried out using a spectroradiometer (Ocean Optics, USB2000+ER). Secondly, the direct photolysis rates of 2NB corresponding to all the aforementioned UV-lights in the photoreactor were monitored using high-performance liquid chromatography (HPLC).[1] Further, the direct emission spectra recorded by the spectroradiometer were scaled until it matched the photon flux needed to achieve observed J_{NB}. Figure S2 shows photon flux spectra ($cm^{-2}s^{-1}nm^{-1}$) for

UVB(Q), UVB(G) and UVA(Q) lights used during aqueous-phase direct photolysis of water-soluble brown carbon (WS-BrC) aerosols in the photoreactor and their comparison with actinic solar photon flux.

Further, we simulated wavelength-dependent direct photolysis rates, referred to as action spectra, of pine wood WS-BrC ($dJ_{WS\text{-}BrC}/d\lambda$) as a case study to assess and compare atmospheric relevance of all three UV-lights with respect to clear-sky actinic solar photon flux of Earth retrieved from Simple Model of Atmospheric Radiative Transfer of Sunshine (SMARTS) program.[3] The $dJ_{WS\text{-}BrC}/d\lambda$, expressed in $sec^{-1}nm^{-1}$, was simulated from 260 to 400 nm using following equation:[1,2]

$$\frac{dJ_{WS-BrC}}{d\lambda}(sec^{-1}nm^{-1}) = I_{\lambda}^{'} \times \phi(\lambda) \times \sigma(\lambda) \quad \text{Eq. S2}$$

where $I_{\lambda}^{'}$ is the photon flux spectrum expressed in photons $cm^{-2}s^{-1}nm^{-1}$ (Figure S2), $\phi(\lambda)$ is quantum yield (molecule $photon^{-1}$) and $\sigma(\lambda)$ is absorption cross-section ($cm^2molecule^{-1}$) of WS-BrC. $\phi(\lambda)$ of 1 was assumed for all photon flux conditions discussed above. $\sigma(\lambda)$ values were based spectrophotometric measurements carried out in this study. Figure S3 shows comparison of action spectra of WS-BrC corresponding to UVB(Q), UVB(G), UVA(Q) and clear-sky actinic solar photon fluxes.

Section S2. Calculation of [OHss] During OH oxidation

Pimelic acid is highly sensitive to ESI^- ionization technique. For quantification of steady-state OH concentration ($[OH_{ss}]$), the aqueous solution of each solid biomass fuel burning sample was spiked with 10 μM pimelic acid and its decay during OH oxidation was monitored using an LC-MS (LTQ XL LC-MS, Thermo Scientific). The decay profiles of pimelic acid during OH oxidation of aqueous solution of all three solid biomass fuel burning samples are shown in Figure S4. The $[OH_{ss}]$ was calculated using following equation:

$$[OHss] = \frac{k^{I}_{decay,\ PA}}{k^{II}_{OH,\ PA}} \quad \text{Eq. S3}$$

where $k^{I}_{decay,\ PA}$, expressed in s^{-1}, is first-order decay constant for pimelic acid degradation during OH oxidation of WS-BrC arising from dung cakes and pine wood burning. $k^{II}_{OH,\ PA}$ is OH radical second-order rate constant of pimelic acid in aqueous medium. In this study, $k^{I}_{decay,\ PA}$ was calculated using methodology above and shown in Figure S4. Moreover, $k^{II}_{OH,\ PA}$value of 2.8×10^9 $M^{-1}s^{-1}$ was taken from a recent study.[4]

Section S3. Total Organic Carbon (TOC) and Total Nitrogen (TN) Measurements

TOC and TN concentration in aqueous extract of particulate laden filters were measured using a TOC analyzer with a TN measurement unit (Shimadzu TOC-L CPH Analyzer). The TOC concentration, referred to as water-soluble organic carbon (WSOC) in this study, was quantified using non-purgeable organic carbon (NPOC) method. In NPOC method, an aliquot of aqueous extracts was acidified with 1M HCl and subsequently sparged to remove purgeable organic (volatile fraction) and inorganic carbon. The remaining carbon in aqueous extract is then converted to carbon dioxide (CO_2) gas and detected by a non-dispersive infrared detector. The NPOC method is more accurate for TOC measurements compared to Total Carbon/Inorganic Carbon method.[5,6] However, loss of volatile organic carbon during the purging may lead to an underestimation of TOC concentrations. For TN measurements, the extract was combusted to NO_X and subsequently reacted with O_3 to form NO_2 in an excited state. Photons emitted by NO_2 during this process were measured by a chemiluminescence detector. The quantitation of WSOC and TN was achieved by calibrating the TOC instrument with known ACS grade standards, *i.e.*, potassium hydrogen phthalate for NPOC, and nitrate salts for TN.

Section S4. Calculation of Solar-weighted Total Absorbance

The comparison of absorption properties of WS-BrC at a single wavelength (*e.g.*, 365 nm) might not be sufficient to understand their photochemical evolution over time.[7,8] Therefore, the solar-weighted total absorbance ($A_{Tot\text{-}(WS\text{-}BrC)\text{-}SW}$) of WS-BrC aerosols emitted from different solid biomass fuel burning types was determined in this study using following equations:

$$A_{(WS-BrC)-SW-\lambda} = A_{WS-BrC-\lambda} \times \frac{S_\lambda}{\int_{330}^{500} S_\lambda d\lambda} \quad \text{Eq. S4}$$

$$A_{Tot-(WS-BrC)-SW} = \int_{330}^{500} A_{(WS-BrC)-SW-\lambda} d\lambda \quad \text{Eq. S5}$$

where $A_{WS\text{-}BrC\text{-}\lambda}$ is WS-BrC absorbance at a given wavelength (λ), $A_{(WS\text{-}BrC)\text{-}SW\text{-}\lambda}$ is solar-weighted absorbance at λ and S_λ is clear sky spectral solar irradiance (W/m^2/nm) on tilted receptor plane at λ and was adopted from Simple Model of Atmospheric Radiative Transfer of Sunshine (SMARTS) program.[3] The above integrations were carried out from 330 to 500 nm using trapezoidal rule [data interval = 1 nm].

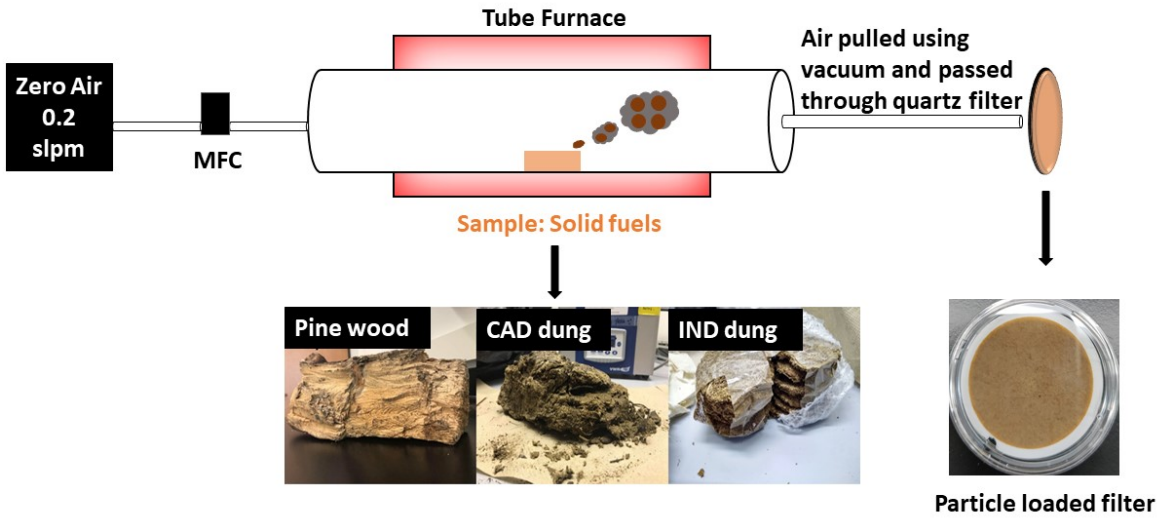

103

104 **Figure S1.** Schematic of the tube furnace set-up along with pictures of solid biomass fuels
105 explored in this study. These solid biomass fuels were pine wood, Indian (IND) dung cakes
106 and Canadian (CAD) dung cakes. Moreover, MFC refers to mass flow controller.

107

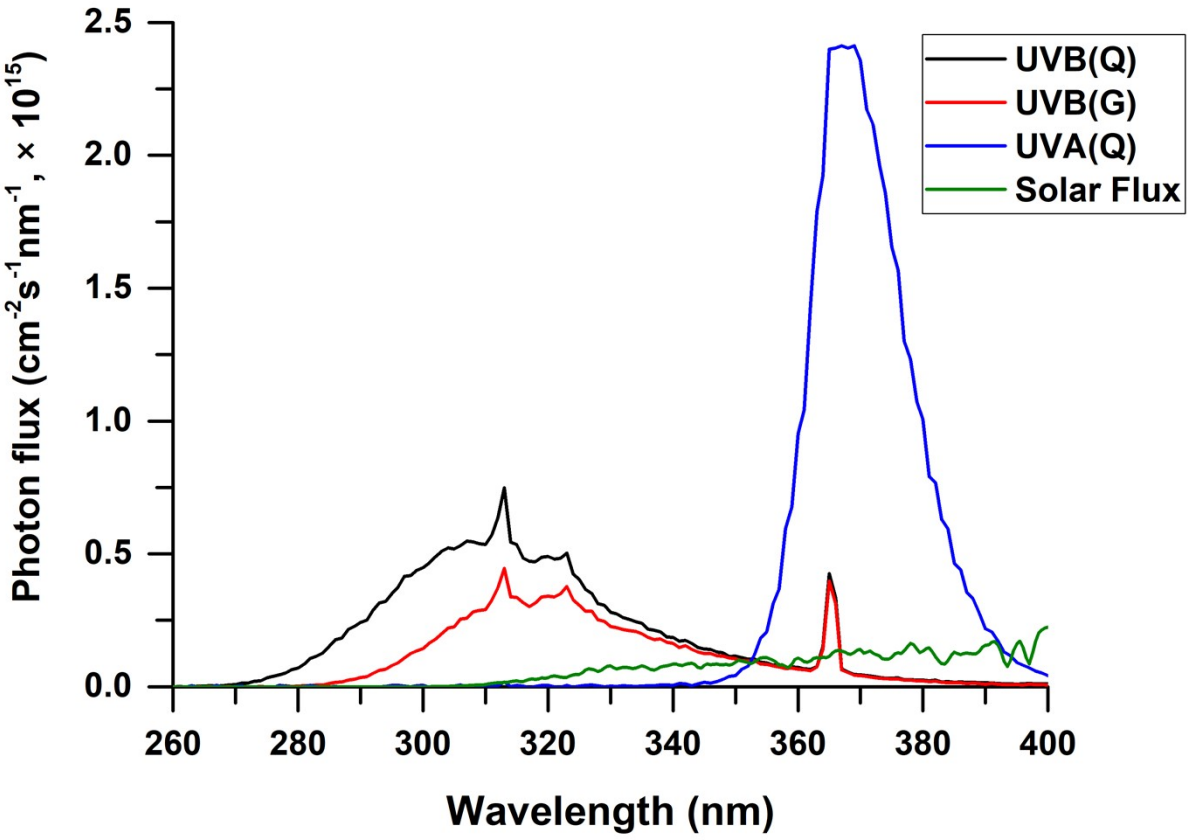

Figure S2. Photon flux spectra ranging from 260 to 400 nm, expressed in cm^{-2} s^{-1} nm^{-1}, of distinct ultraviolet (UV) lamps utilized during aqueous-phase direct photolysis of WS-BrC aerosols in the photoreactor and their comparison with actinic solar photon flux. Here, UVB(Q) and UVB(G) indicate UVB spectrum in quartz and glass vessel, respectively. UVA(Q) indicates UVA spectrum in quartz vessel. The actinic solar photon flux spectrum is based on Simple Model of Atmospheric Radiative Transfer of Sunshine (SMARTS) program.[3]

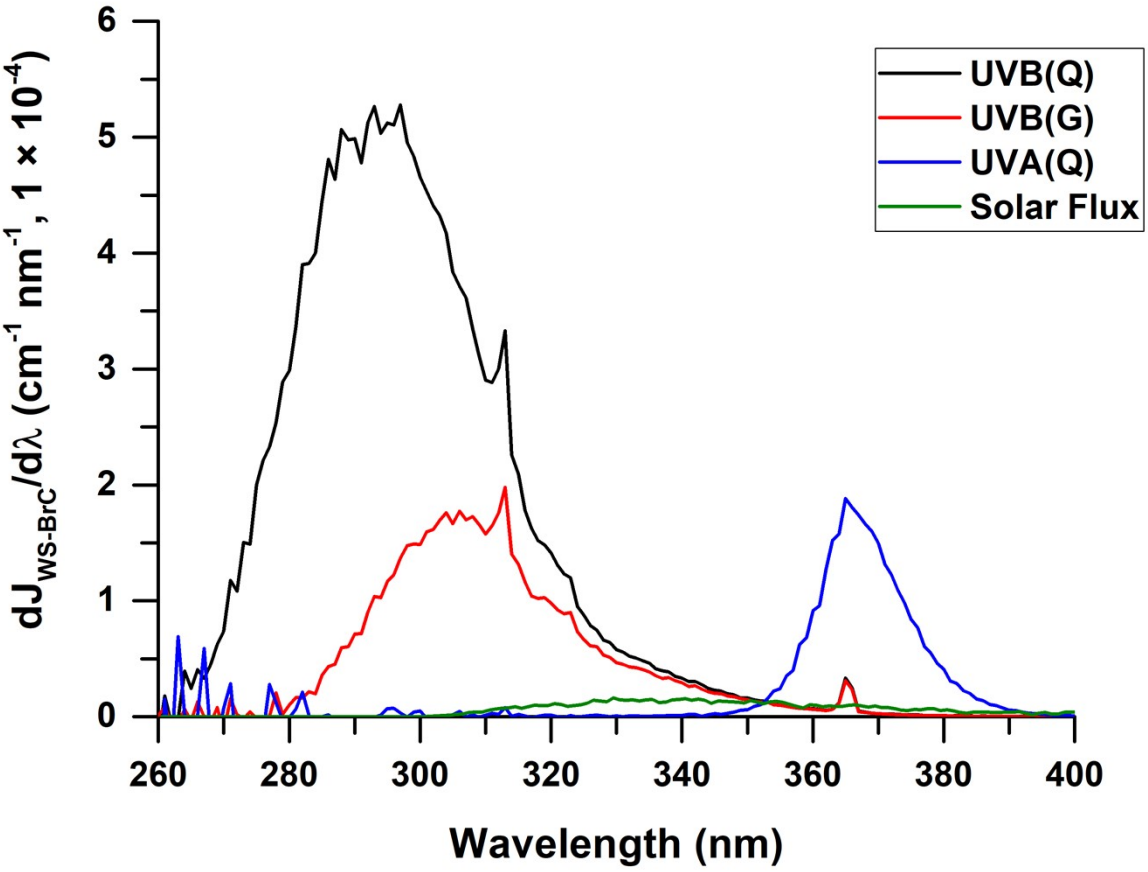

116

117 **Figure S3.** Comparison of action spectra, simulated for UVB(Q), UVB(G), UVA(Q) and clear-
118 sky actinic solar photon flux ranging from 260 to 400 nm, of WS-BrC ($dJ_{WS-BrC}/d\lambda$) arising
119 from pine wood burning.

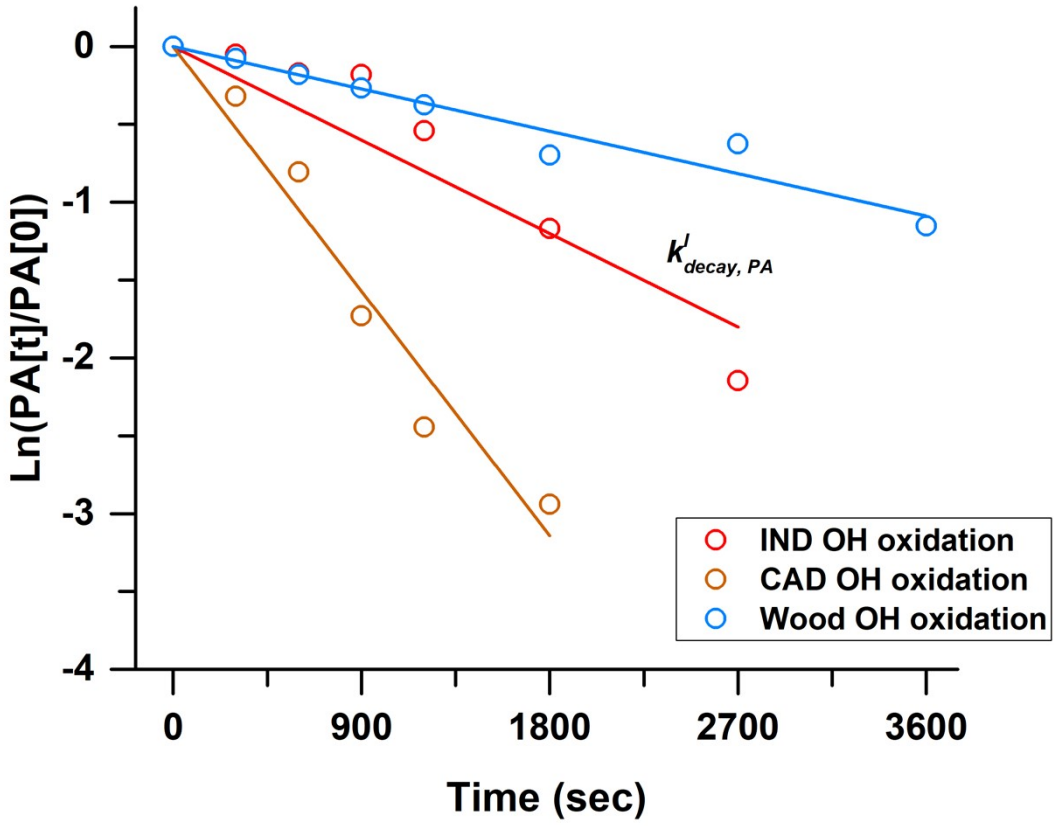

120

121 **Figure S4.** Photochemical decay profile of pimelic acid (PA), expressed by temporal change
122 in pimelic acid intensity normalized to its initial value on logarithm scale (Ln(PA[t]/PA[0])),
123 during OH oxidation of WS-BrC arising from IND dung, CAD dung and pine wood burning.
124 Where, $k^{I}_{decay,\ PA}$ indicate first-order decay constant obtained by linear regression fit of the
125 decay profile.

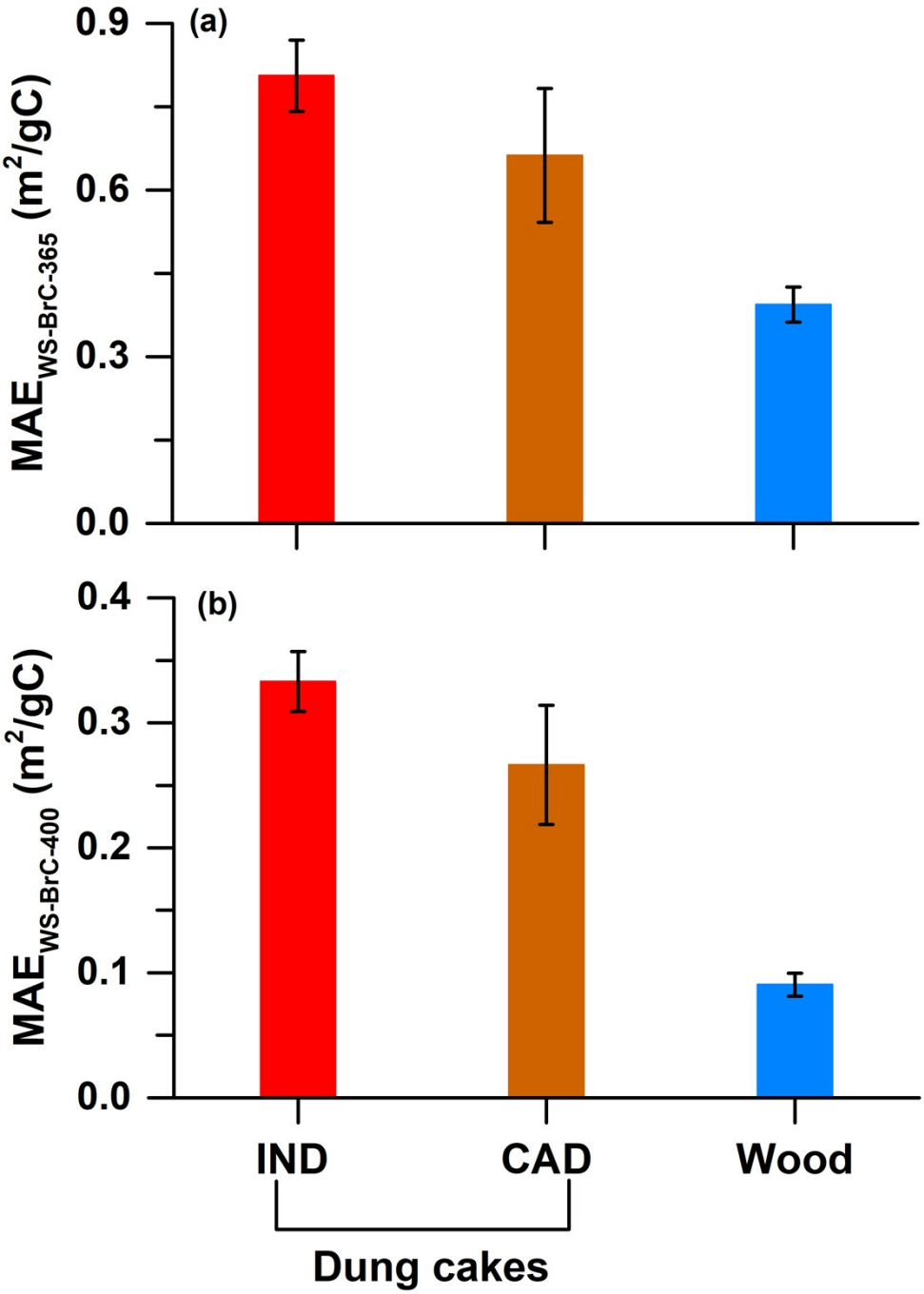

126

127 **Figure S5.** Mass absorption efficiency of WS-BrC ($MAE_{WS\text{-}BrC\text{-}365}$) arising from dung cakes

128 (from India (IND) and Canada (CAD)) and pine wood burning at: (a) 365 nm and (b) 400 nm.

129

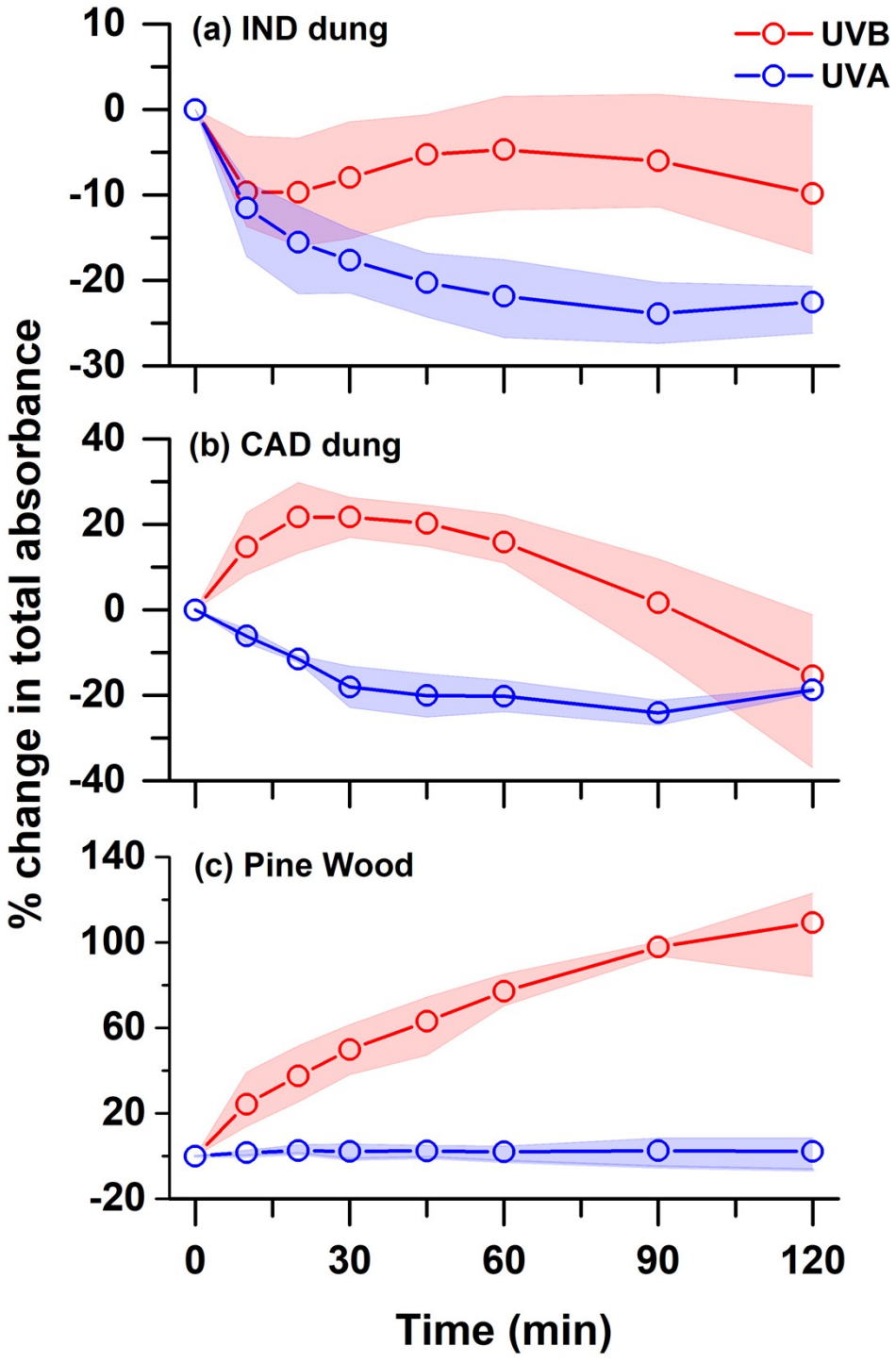

Figure S6. Temporal variability of % change in solar-weighted total absorbance of WS-BrC aerosols emitted from (a) IND dung, (b) CAD dung and (c) Pine wood burning during their direct photolysis using UVB(Q) and UVA(Q) light. Where, (Q) denotes that the experiments were performed in a quartz vessel

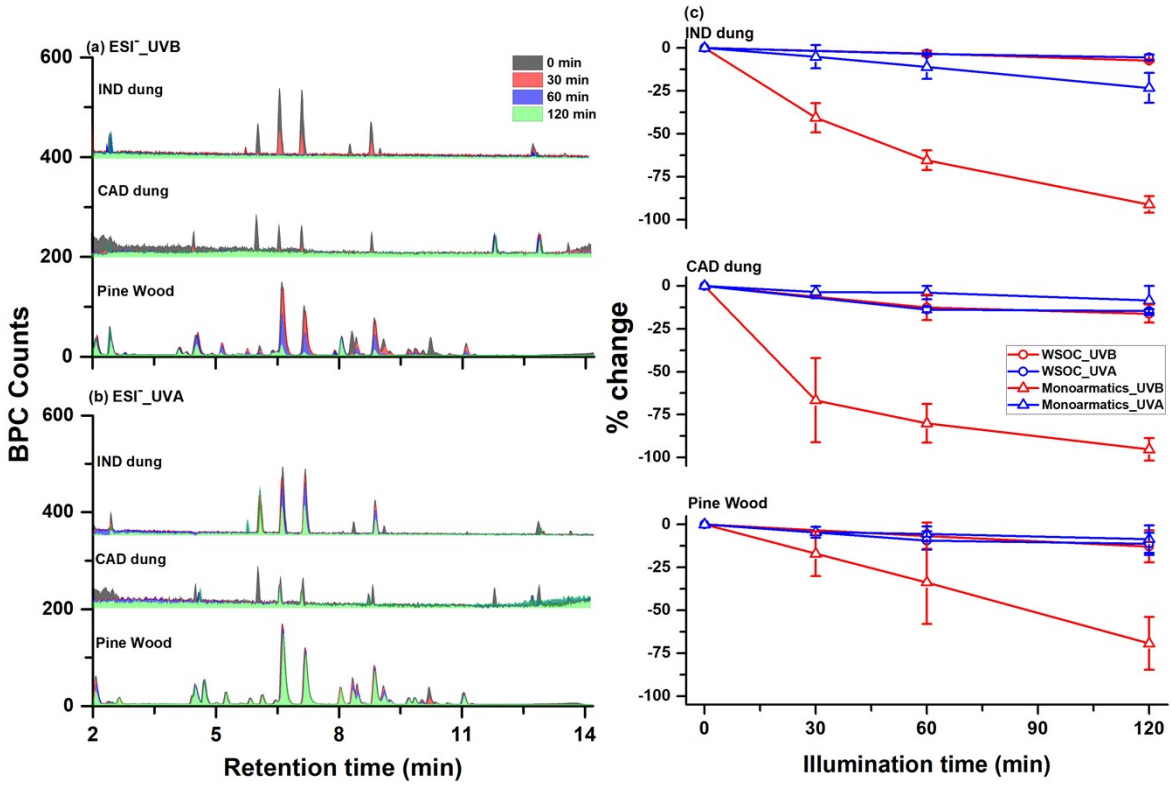

Figure S7. Temporal variation in ESI^- LC-MS BPC chromatogram of water-soluble organics upon exposure to UVB(Q) and UVA(Q)-light during aqueous-phase direct photolysis (a, b) and % change in net intensity of monoaromatic compounds along with WSOC concentrations (c) for all three solid biomass fuel burning types.

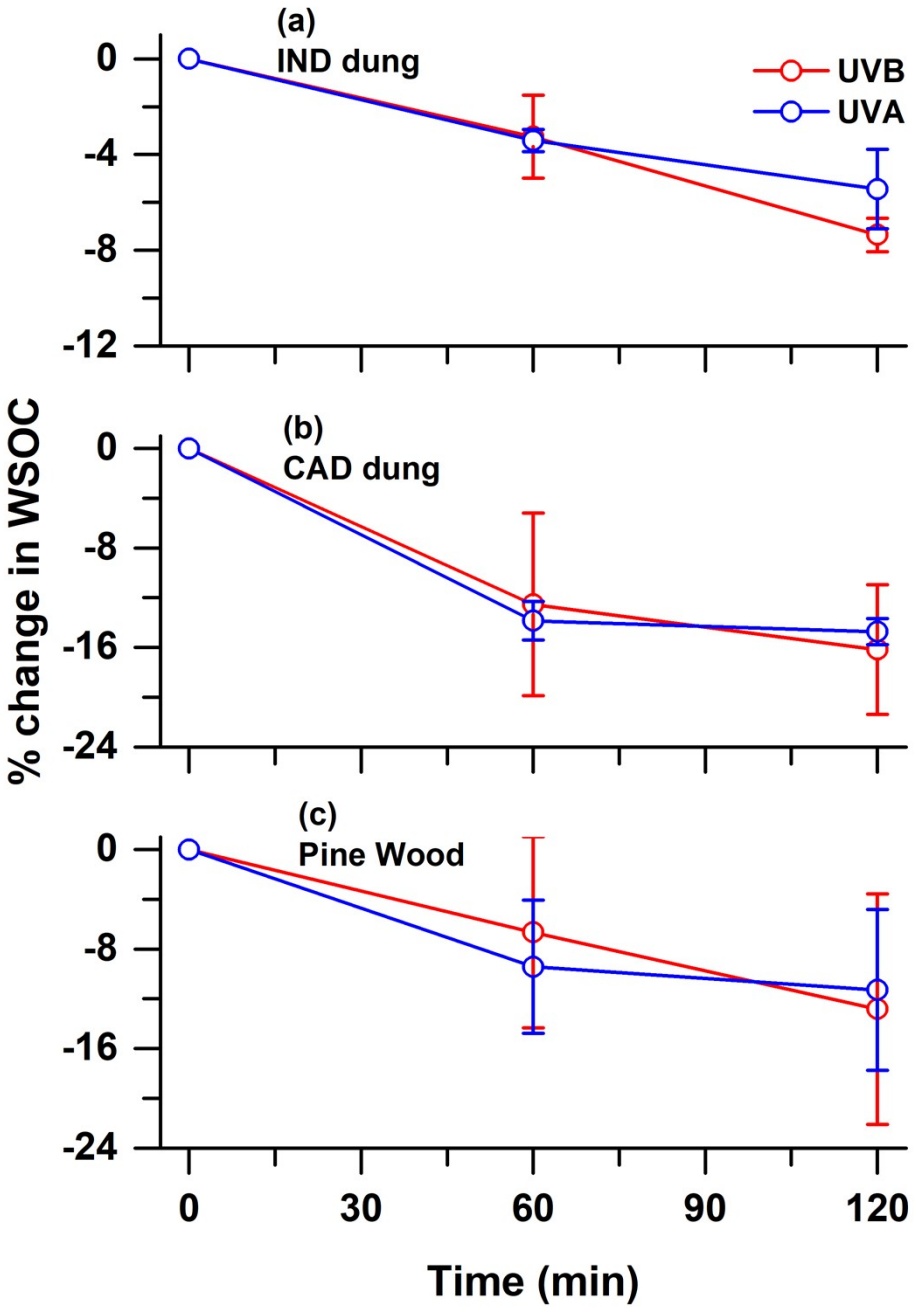

143

144 **Figure S8.** Temporal variation of % change in WSOC concentration during the direct
145 photolysis using UVB(Q) and UVA(Q) light for (a) IND dung, (b) CAD dung and (c) Pine
146 wood burning.

147

148

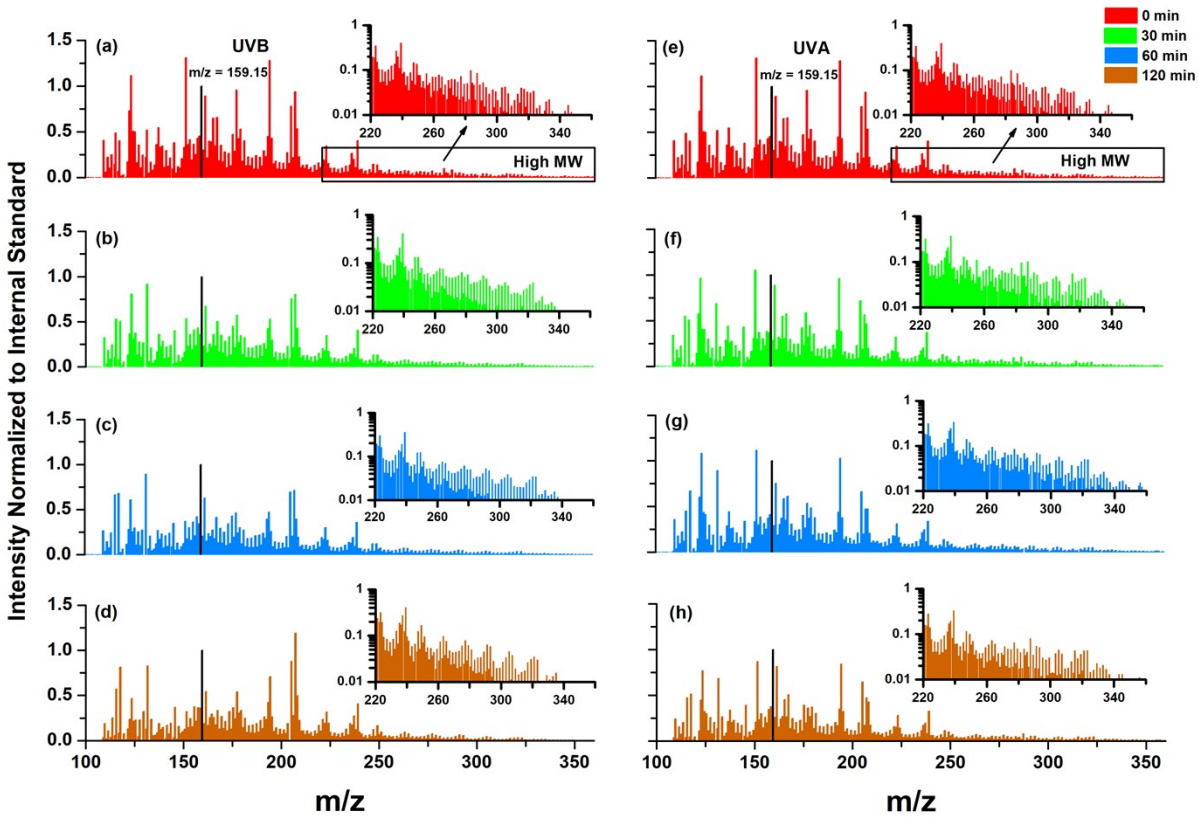

Figure S9. Internal standard normalized direct flow-injection MS injection spectra at 0, 30, 60 and 120 min for pine wood burning during UVB(Q) and UVA(Q) direct photolysis experiments. Here, black bar is normalized signal for internal standard (*i.e.*, pimelic acid, m/z = 159.15).

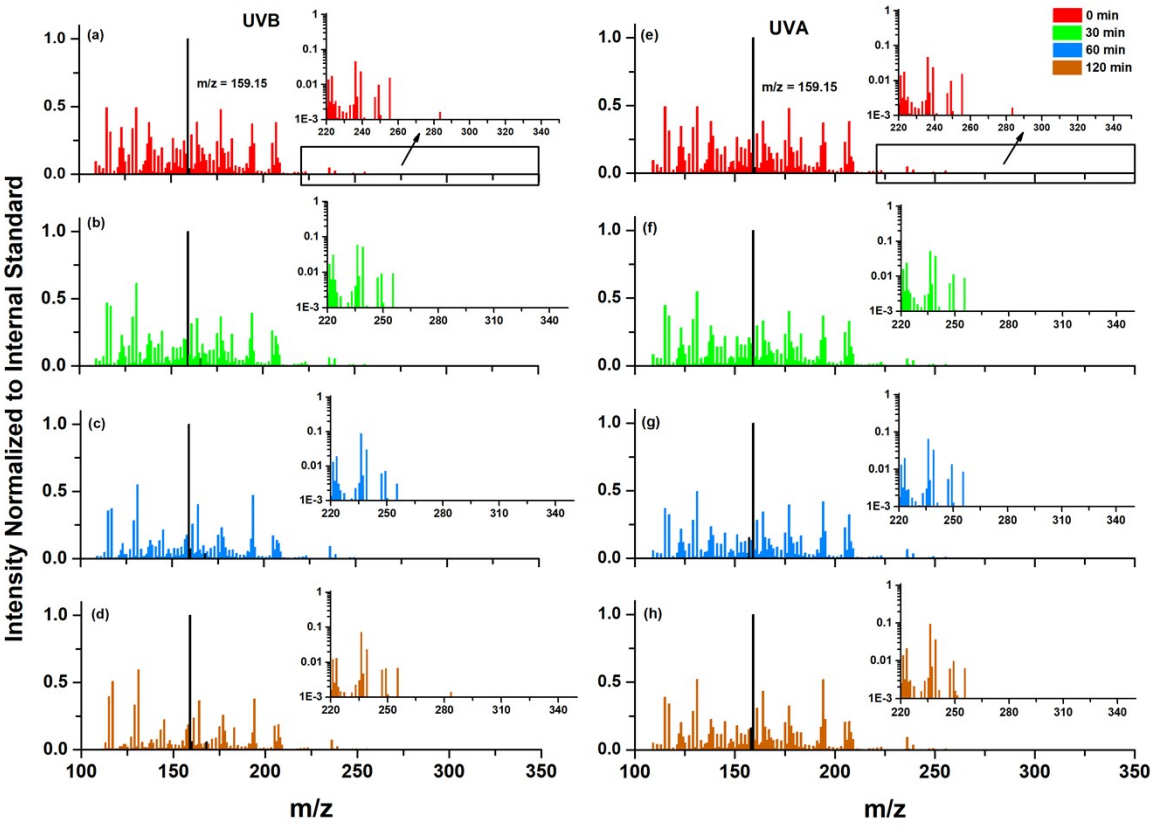

155

156 **Figure S10.** Internal standard normalized direct flow-injection MS injection spectra at 0, 30,
157 60 and 120 min for IND dung burning samples during UVB(Q) and UVA(Q) aqueous-phase
158 direct photolysis experiments. Here, black bar is normalized signal for internal standard (*i.e.*,
159 pimelic acid, m/z = 159.15).

160

161

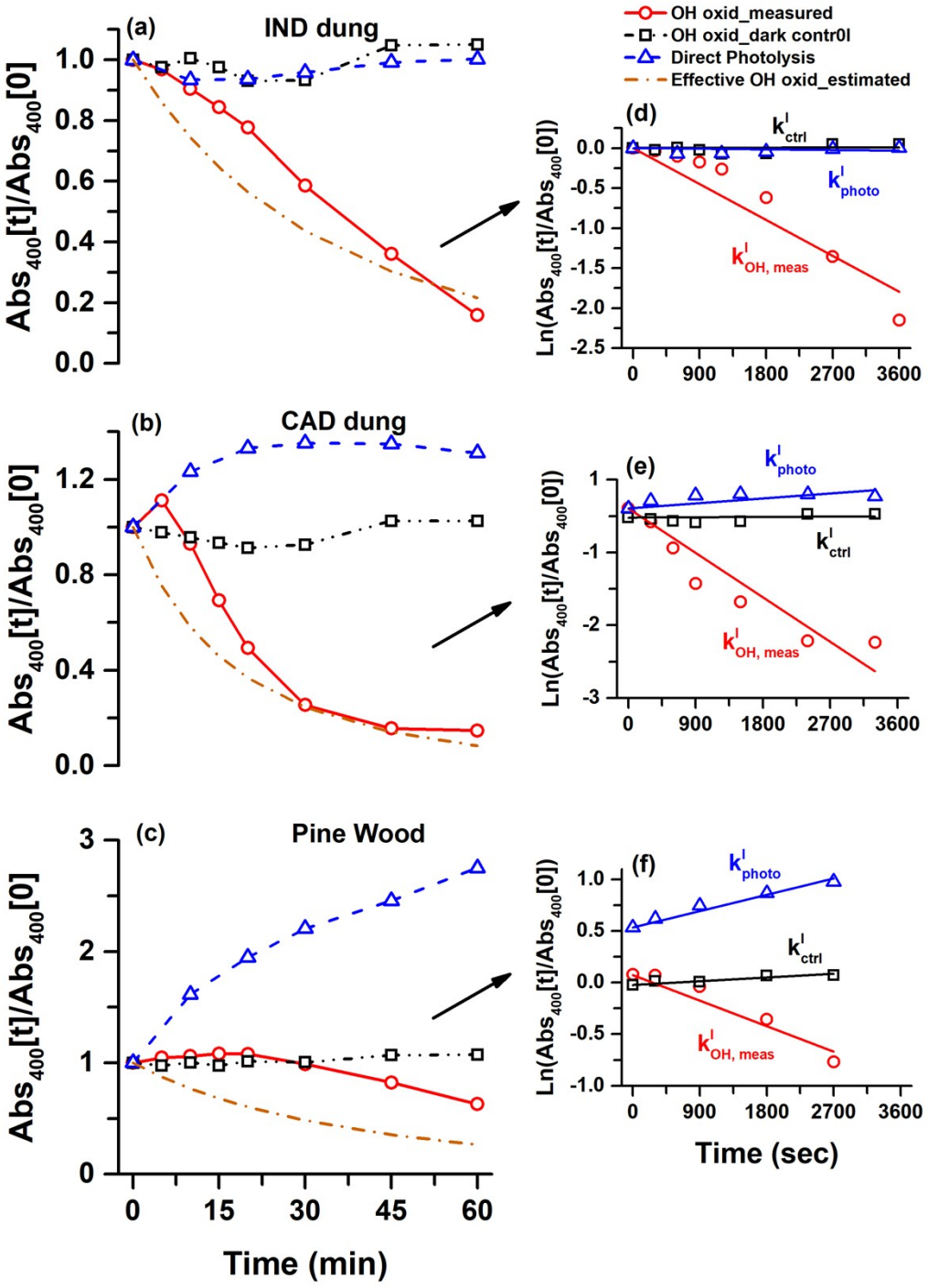

Figure S11. Temporal profiles of absorbance at 400 nm normalized to initial value ($Abs_{400}[t]/Abs_{400}[0]$) during aqueous-phase OH oxidation (red), dark control (black) and direct photolysis (blue) experiments for WS-BrC emitted from IND dung (a, d), CAD dung (b, e) and pine wood burning (c, f). The plots (a), (b) and (c) indicate photochemical decay/enhancement profile of $Abs_{400}[t]/Abs_{400}[0]$, whereas (d), (e), and (f) indicate corresponding first-order

decay/enhancement plots for WS-BrC. The maximum absorbance datapoint was considered as origin for determination of first order-decay constant. Moreover, the brown color dashed lines represent effective OH oxidation

Table S1. High-resolution ESI^- LC-MS analysis of mixture of five known standard compounds.

Compound Name	**Chemical formula**	**Calculated Mass to Charge (m/z)***	**Intensity**
Vanillin	$C_8H_8O_3$	151.04	1.66×10^4
Sinapaldehyde	$C_{11}H_{12}O_4$	207.07	4.24×10^4
Coniferyl aldehyde	$C_{10}H_{10}O_3$	177.06	6.88×10^4
4-Nitroguaiacol	$C_7H_7NO_4$	168.03	3.20×10^5
4-Nitrocatechol	$C_6H_5NO_4$	154.01	5.16×10^5

All these standard compounds are commonly observed in biomass burning smoke.[9]

*Assigned by MassHunter software

Table S2. WSOC and TN concentrations for different types of solid biomass fuel burning.

Fuel type	Parameters*			
	WSOC (mg-C/L)	**TN (mg-N/L)**	**TIN$ (µg-N/L**	**WSON/WSOC&**
Blanks [a, c]	3.8 ± 0.1	0.37 ± 0.07	< LOD	-
IND dung [#, b, d]	139.7 ± 30.2	10.65 ± 2.05	< LOD	0.077 ± 0.004
CAD dung [#, a, e]	34.2 ± 4.5	3.90 ± 1.55	-	0.115 ± 0.047
Pine Wood [#, b, e]	403.6 ± 300.4	5.85 ± 4.44	<LOD	0.015 ± 0.006

* Mean ± standard deviation; # all values are blank corrected; WSOC = water-soluble organic carbon; TN = total nitrogen (water-soluble); TIN = total inorganic nitrogen (water-soluble); WSON = water-soluble organic nitrogen

$ TIN = $(NO_2^- - N + NO_3^- - N)$. Measured using colorimetric autoanalyzer (ThermoFisher Gallery Beermaster Plus). Limit of detection (LOD) = 4.3 µg/L

& Since, inorganic nitrogen constituents (e.g., NO_2^-, NO_3^-) are negligible compared to TN. Therefore, TN/WSOC ratio (i.e., organic + inorganic fraction) would likely to reflect more closely with water-soluble organic nitrogen fraction (i.e., WSON/WSOC) than inorganic fraction.

[a] extracted in 25 mL; [b] extracted in 30 mL (diluted by 8 times during WSOC, TN and TIN measurements)

[c] n = 2; [d] n = 3; [e] n = 4

Table S3. Molecular composition details of monoaromatic compounds found in water-extracts of dung cakes and pine wood burning samples using high-resolution ESI^- LC-MS analysis.

Calculated Mass to Charge (m/z)	Molecular Formula	Possible Identity	IND	CAD	Wood
109.0296	$C_6H_6O_2$	Catechol	Y	Y	Y
121.0298	$C_7H_6O_2$	Benzoic acid	Y	N	Y
123.0453	$C_7H_8O_2$	Guaiacol	Y	Y	Y
125.0246	$C_6H_6O_3$	Isomaltol	Y	N	Y
135.0454	$C_8H_8O_2$	-	Y	Y	Y
137.0609	$C_8H_{10}O_2$	1, 2-Dimethoxybenzene	Y	N	Y
149.0610	$C_9H_{10}O_2$	4-Ethylbenzoic acid	Y	N	Y
151.0401	$C_8H_8O_3$	Vanillin	Y	Y	Y
151.0767	$C_9H_{12}O_2$	-	Y	N	Y
155.0351	$C_7H_8O_4$	-	Y	N	Y
166.0514	$C_8H_9NO_3$	4-Nitrophenethyl alcohol	Y	N	N
177.0559	$C_{10}H_{10}O_3$	Coniferyl aldehyde	Y	Y	Y
181.0515	$C_9H_{10}O_4$	Syringaldehyde	Y	N	Y
195.0667	$C_{10}H_{12}O_4$	Trimethoxy benzaldehyde	Y	N	N

Where, Y indicates that specie was identified in ESI^- LC-MS spectra; N indicates that specie couldn't identified.

Table S4. Temporal variation in ratio of internal standard normalized total intensity of high molecular-weight compounds to low molecular-weight compounds during aqueous-phase UVB(Q) and UVA(Q) direct photolysis of pine wood burning water-soluble organics.

Exposure time (min)	Pine wood	
	UVB*	UVA*
0	0.141 ± 0.078	0.189 ± 0.092
30	0.151 ± 0.091	0.156 ± 0.081
60	0.155 ± 0.090	0.169 ± 0.079
120	0.172 ± 0.103	0.166 ± 0.069

Where, m/z = 215 to 350 were considered high molecular-weight compounds (dimer range); m/z = 100 to 215 were taken as low molecular-weight compounds (monomer range); 20μM pimelic acid was used as internal standard.

* Results are average of direct flow-injection MS analysis of two pine wood burning filter water-extracts

Table S5. Comparison of average intensity of a few monoaromatics compounds in water-extracts of IND dung and pine wood burning samples.

Compound Name	**Intensity***	
	IND dung	**Pine wood**
Guaiacol	127.4	201.2
Vanillin	19.3	28.0
Coniferyl aldehyde	16.0	54.3

* Normalized to average WSOC concentration of respective solid biomass fuel burning

Table S6. Aqueous-Phase second-order rate constants and estimated cloud-water half-life of WS-BrC emitted from pyrolysis of different solid biomass fuels, calculated from absorbance at 400 nm.

Origin/Type	$k_{OH,\ meas}^{II}$ **&** ($M^{-1}\ s^{-1}$; × 10^8)	$k_{OH,\ eff}^{II}$ **$** ($M^{-1}\ s^{-1}$; × 10^8)	$\tau_{1/2,\ cloud\text{-}water}$ **#** (min)
IND dung	29.1 ± 3.7	28.4 ± 1.4	59 ± 3
CAD dung	19.0 ± 14.8	20.2 ± 15.2	138 ± 83
Pine Wood	15.9 ± 4.3	40.4 ± 12.5	45 ± 14

& Corrected for dark (H_2O_2) control.

$ Corrected for contribution due to dark control and UVB direct photolysis.

Estimated corresponding $k_{OH,\ eff}^{II}$ and by assuming an ambient cloud water with [OH]ss of 1 × 10^{-13}M, representing upper band of OH in remote cloud-waters.[10]

References

1 E. S. Galbavy, K. Ram and C. Anastasio, 2-Nitrobenzaldehyde as a chemical actinometer for solution and ice photochemistry, *J. Photochem. Photobiol. A Chem.*, 2010, **209**, 186–192.

2 J. V. Amorim, S. Wu, K. Klimchuk, C. Lau, F. J. Williams, Y. Huang and R. Zhao, PH Dependence of the OH Reactivity of Organic Acids in the Aqueous Phase, *Environ. Sci. Technol.*, 2020, **54**, 12484–12492.

3 C. A. Gueymard, SMARTS2, a simple models of the atmospheric radiative transfer of sunshine, *Florida Sol. Energy Center/University Cent. Florida*, 1995, 84.

4 T. Schaefer, L. Wen, A. Estelmann, J. Maak and H. Herrmann, pH-and temperature-dependent kinetics of the oxidation reactions of OH with succinic and pimelic acid in aqueous solution, *Atmosphere (Basel).*, 2020, **11**, 17–24.

5 K. Yang and B. Xing, Adsorption of fulvic acid by carbon nanotubes from water, *Environ. Pollut.*, 2009, **157**, 1095–1100.

6 I. Bisutti, I. Hilke and M. Raessler, Determination of total organic carbon - An overview of current methods, *TrAC - Trends Anal. Chem.*, 2004, **23**, 716–726.

7 V. Choudhary, P. Rajput and T. Gupta, Absorption properties and forcing efficiency of light-absorbing water-soluble organic aerosols: Seasonal and spatial variability, *Environ. Pollut.*, 2021, **272**, 115932.

8 D. Sengupta, V. Samburova, C. Bhattarai, E. Kirillova, L. Mazzoleni, M. Iaukea-Lum, A. Watts, H. Moosmüller and A. Khlystov, Light absorption by polar and non-polar aerosol compounds from laboratory biomass combustion, *Atmos. Chem. Phys.*, 2018, **18**, 10849–10867.

9 M. Loebel Roson, R. Duruisseau-Kuntz, M. Wang, K. Klimchuk, R. J. Abel, J. J. Harynuk and R. Zhao, Chemical Characterization of Emissions Arising from Solid Fuel Combustion - Contrasting Wood and Cow Dung Burning, *ACS Earth Sp. Chem.*, 2021, **5**, 2925–2937.

10 H. Herrmann, D. Hoffmann, T. Schaefer, P. Bräuer and A. Tilgner, Tropospheric aqueous-phase free-radical chemistry: Radical sources, spectra, reaction kinetics and prediction tools, *ChemPhysChem*, 2010, **11**, 3796–3822.